BaBiO$_3$ Assisted Photodegradation of Malachite Green Dye Under Visible Light Irradiation: Adsorption and Degradation Kinetics

K. Sharma*, S. Jain, U. Chandrawat

Department of Chemistry, Govt. P.G. College, Kota 324001, India

ABSTRACT

Nano sized BaBiO$_3$ is prepared through Pechini method and characterized by SEM, XRD, FTIR, DT-TGA and UV DRS. The kinetic studies of adsorption and degradation phenomena involved in the photocatalytic degradation of Malachite Green dye using a batch reactor under visible light were investigated. Experiments were performed in a suspended BaBiO$_3$ photocatalyst system. The effect of catalyst loading, solution pH and initial dye concentration on dye degradation is investigated. In addition, adsorption experiment is also performed which indicates that adsorption pattern follows Langmuir model. The decomposition of Malachite Green dye follows pseudo first order kinetics and the Langmuir-Hinshelwood mechanism is found to be valid. Different kinetic parameters for adsorption and photocatalytic degradation of dye are also determined.

doi: 10.5829/idosi.ijee.2016.07.03.10

INTRODUCTION

The industrial and textile wastewater is a considerable source of non-aesthetic pollution in the environment and can create dangerous byproducts through oxidation, hydrolysis or other chemical reactions that take place in the wastewater phase [1-2]. The presence of small amount of dyes is clearly visible and considerably influences the water ecosystem.

Amongst the different pollutants from the textile industry, Malachite Green (MG) is the one of the main disastrous pollutant[3-4]. The use of this dye has been banned in several countries and is not approved by US Food and Drug Administration; it is still being used in many parts of the world due to its low cost, ready availability and efficacy [5].

MG degradation has been studied by various biological and physiochemical methods [6-7]. However, these treatment methods only provide separation of the dyes without any dye degradation, creating a waste disposal problem with the large quantities of sludge production. To resolve this problem, advanced oxidation processes based on heterogeneous catalysis techniques

are being used for the degradation of MG. In several studies TiO$_2$ is used predominantly due to its low cost and non toxicity [8-9]. However, photochemical efficiency of TiO$_2$ is limited to UV region only, due to its wide band gap [3.2eV]. Various modifications including cation and anion doping, coupling with semiconductors have been used to enhance photoabsorption ability of TiO$_2$ in visible region[10-11]. These modified samples of TiO$_2$ show good photocatalytic activity in visible region, but their activity is not high enough for practical application because of their less stability [12]. Also, sometimes these modifications may cause the distortion of band structure and these additional elements act as a scattering centre which further leads to decrease in photocatalytic activity [13]. Therefore, developing a visible light active photocatalytic material is essential for practical application of photocatalytic technology at wide range. The energy gap of perovskite [14-15] is usually less than 3.0 eV hence it shows good photocatalytic activity in visible light region. Recently, Bismuth based visible light active perovskites such as LiBiO$_3$[16], KBiO$_3$ [16], AgBiO$_3$ [17] are prepared by hydrothermal synthesis and solvent thermal synthesis respectively. In this paper, we

* Corresponding author: Kavita Sharma
E-mail: kavi21089.sharma@gmail.com
Tel- +919461391230

present a simple Pechini type [18] polymerizable complex route, based on polyesterification between citric acid and ethylene glycol that has been successfully used to synthesize several other compounds with perovskite structure [19-20]. Sol-Gel method is advantageous compared to other processing methods, as it allows control over size, calcinations temperature and also it provides chemically uniform powders. The prepared catalyst is characterized by XRD, SEM, UV-DRS, FTIR for structural determination. The photocatalytic activity of thus prepared sample has been evaluated via the degradation of MG dye in aqueous solution under visible irradiation. The initial rates of the reaction are calculated for various initial dye concentrations. The Langmuir-Hinshelwood model [21-22] is found suitable for interpreting the initial rate data and for the development of a rate equation for degradation of MG dye. An adsorption study of $BaBiO_3$ has also been discussed.

MATERIAL AND METHODS

Materials
In this study all chemicals used are of analytical reagent grade. Barium nitrate, Bismuth nitrate, citric acid and ethylene glycol are purchased from Merck (India). Malachite green is obtained from SDS Fine Chem. (P.) Ltd.(India). Deionised water purified with a milli-Q-water ion exchange system (Millipore Co.) is used throughout the study. Chemical structure of malachite green dye is depicted below-
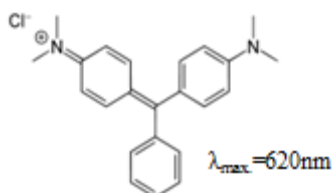

Figure 1. Structure of Malachite Green dye

Preparation of $BaBiO_3$ perovskite
$BaBiO_3$ perovskite is prepared by the sol-gel route [Pechini method][17]. Barium nitrate and bismuth nitrate are firstly dissolved in doubly distilled water and dil HNO_3 respectively to get 1.0M solution each. These two are used as starting materials. Both the above solutions are mixed and then magnetically stirred to get a uniform solution. After addition of 1M citric acid [CA] to above solution stirring is performed up to 30 minutes followed by addition of ethylene glycol [EG]. Here, CA and EG are used as complexing agents. The molar ratio among Barium, Bismuth cations is 1:1. The CA/metal ratio is fixed at 4.0 while keeping the CA/EG ratio as 60/40.Thus obtained solution is transferred to a hot plate where it is heated upto 90ºC resulting in the formation of brown

resin. This resin is pulverised and then calcined at 850º C for 12 hours to obtain $BaBiO_3$ Perovskite.

Characterization
Ex-star 6300 thermal analyzer is used to make thermogravimetric (TGA) and differential thermoanalytic (DTA) measurements in air flow (200 mL min⁻¹) in the temperature range 31-900 ºC with a heating rate of 5 ºC min⁻¹. The structural characterization is done by X-ray diffraction using a X-ray diffractrometer [Siemens D500] equipped with a high intensity CuKα radiation, and operated at 45kV and 40mA accelerating voltage and the applied current, respectively. A scan rate of 5º min⁻¹were used for 0-90º 2θ values. The morphology and particle size are analyzed using Scanning electron microscope [HitachiX650, Japan]. Fourier transform infrared (FTIR) [Spectrum 100, Perkin Elmer] is utilized to identify chemical bonds existed in the powder.UV-DRS spectrum is carried out using Schimadzu Lambda 900 Spectrophotometer. The spectrum is recorded at 240-800 nm wavelengths.

Catalytic activity
The adsorption experiments in dark are carried out in order to evaluate the equilibrium constant of adsorption. Stock solutions of the different initial dye concentration (C_0) are prepared. A fixed amount of the adsorbent (0.1gram) is added to the 100 mL of above solution. The flasks are then agitated simultaneously for 2h at room temperature. The suspension is centrifuged in order to remove $BaBiO_3$ catalyst. The amount of adsorbate uptake q_e (mgg⁻¹) can be calculated as-

$$q_e = (C_0 - C_e) \, V/ \, W \times 100 \qquad (1)$$

where C_0 is the initial adsorbate concentration (mgL⁻¹); C_e is the equilibrium concentration in solute on (mgL⁻¹); V is the volume of solution (L);W is the mass of the adsorbent (g); and q_e is the amount adsorbed(mgg⁻¹).

The visible light irradiation experiments are carried out in an indigenously prepared immersion type photocatalytic reactor. A 500W Xe arc lamp (intensity=137 mWcm⁻²) is used as a visible light source. This lamp is placed in a quartz tube which is sealed from one side. This tube is then immersed in a cylindrical borosilicate reactor (capacity 1 L). In this,mixture of catalyst and dye solution are taken following which the mixture is placed in a water bath circulated at a constant speed to keep the above suspension homogenous. Different dye solutions of various concentrations are made from the stock solution (100 mgL⁻¹) by appropriate dilutions. Before irradiation, the suspensions are magnetically stirred in the dark for 20 minutes to get an adsorption-desorption equilibrium between the catalyst and dye solution.The equilibrium concentration of the dye (C_{eq}) in contact with the catalyst, instead of that of

the feed dye solution, represents the true dye concentration in solution at the start of irradiation. For this reason C_{eq} has been used as C_o for the photodegradation kinetics. The pH of the solutions is adjusted using 0.1N NaOH and 0.1N HCl.

The decrease in absorbance of the dye solution at the characteristic wavelength is observed by taking out the samples at regular intervals throughout the complete experimental run. The aliquots are centrifuged and filtered through Whatman filter paper (No. 42) to remove the catalyst.

The residual dye concentration in the samples are determined using a Systronics double beam UV-VIS spectrophotometer 2203. After that, the absorbance corresponding to the $\lambda_{max.}= 620nm$ are converted to the residual concentration using the predetermined calibration curves for MG dye. Also, the degradation efficiency of the dye at any time t is calculated using the following formula

$$Degradation \% = C_o\text{-}C_t/\ C_o \times 100 \qquad (2)$$

where C_0= concentration of dye solution before photoirradiation (mg L^{-1}), C_t= Concentration of dye solution after photoirradiation (mg L^{-1}).

Blank experiments with the pure dye solution (no addition of catalyst) with constant stirring under visible light irradiation for 30 minutes, are conducted prior to the photocatalytic experiments. No significant degradation of the solution is observed indicating that the direct photolysis of the dye is negligible.

RESULTS AND DISCUSSION

Characterization of catalyst

Fig. 2 shows the DTA- TG analysis curves of the $BaBiO_3$ precursor resin. It can be see that the decomposition of $BaBiO_3$ precursor resin takes place in three distinct steps. The first weight loss region (31-185 ℃) corresponds to the loss of physio-absorbed water and accompanied by 8.9% weight. The second weight loss (60.80%) region is in temperature range of 186-416 ℃, which can be attributed to the pyrolysis and combustion of organic compounds and the degradation of intermediate species formed during the polymerisation process. The next weight loss around 13.0% lies in the range of 417-440℃ and can be attributed to the decomposition of nitrates and nitrites residue. The DTA curve shows three weak exothermic peaks at 200, 259, 292 ℃ and one strong exothermic peak at 456 ℃, which are correlated to the weight loss mentioned above and subsequent crystallization of the residual amorphous phase. This observation is supported by powder X-ray diffraction (XRD) of the sample obtained from calcinations of the precursor at 350, 650 and 800 ℃. (Fig. 3)
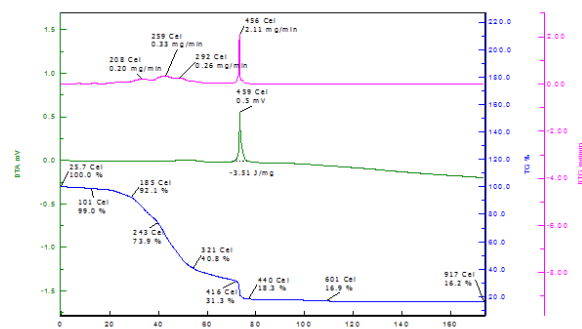

Figure 2. TGA/DTA curves showing thermal decomposition of precursor to a stable $BaBiO_3$

Fig. 3 shows XRD patterns of the samples which were calcined at different temperature 300℃(a), 600℃(b) and 800℃(c). The XRD pattern (a) at 350 ℃ is found to be amorphous in nature as no sharp peak is observed in the diffraction pattern. At 600 ℃,the crystalline perovskite type structure of $BaBiO_3$ started to form and the degree of crystallinity increased with increasing the calcinations temperature as shown in Fig. 3 (b). It is evident from Fig.3 (c) that at 800 ℃ fully crystallized single-phase oxide $BaBiO_3$ with well pronounced perovskite crystal structure has formed and its diffraction peaks corresponds to a monoclinic structure with the lattice parameters a=6.183 Å , b=6.13 Å , c=8.666 Å. (JCPDS 35-1020). The main diffraction peaks are observed at 2θ =29.23°, 45.00°, 51.67° and 59.90°, which is similar to the previously reported data for $BaBiO_3$[23].
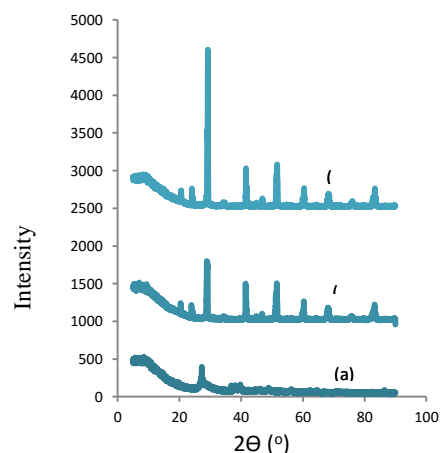

Figure 3. XRD patterns of $BaBiO_3$ (a) at 350°C (b) at 600°C (c) at 800°C

The diffuse reflectance spectra of $BaBiO_3$ (Fig. 4) shows a strong fundamental absorption edge at 600nm, which indicates the photocatalytic activity in the visible light as well as the solar light. Further, the optical band gap E_g was determined from Tauc's formula, i.e.

$$(\alpha E)^2 = A (E - E_g) \qquad (3)$$

where $\alpha = 4\pi\kappa/\lambda$ is the absorption coefficient, E is the photon energy, and A is a constant. The E_g values are determined by extrapolating the linear portion of the plot relating $(\alpha h\nu)^2$ [Kubelka-Munk Function] [24] versus $h\nu$ to $(\alpha h\nu)^2 = 0$ [Kubelka- Munk conversion spectrum]. The optical band gap is estimated to be about 2.07 eV from the onset of the absorption edge.
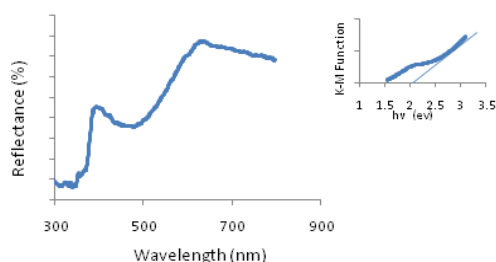

Figure 4.Kubelka-Munk conversion spectrum of $BaBiO_3$.The inset shows an estimation of band gap energy by extrapolation method.

SEM micrographs of $BaBiO_3$ (Fig. 5) show that the nanorods with average width 520nm and length as small as 2.55μm are synthesized by the calcination at 800ºC. This nanosize is further confirmed by the small width of XRD peaks (Fig. 3 c)
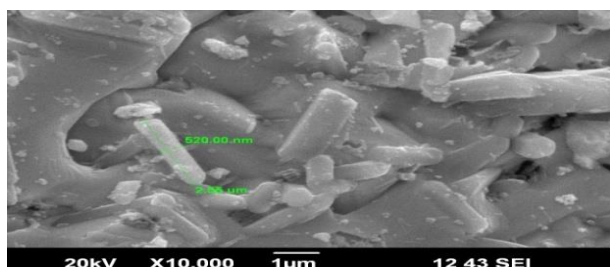

Figure 5.SEM micrographs of $BaBiO_3$ at 1μ magnification

Fig.6 shows the FTIR spectra of the $BaBiO_3$ powder in the range of 400-3500 cm^{-1}, calcined at 800ºC. The FTIR is similar to the most other ABO_3-type perovskite compounds which have common BO_6 oxygen-octahedral structure. [25]The band at nearly 468 cm^{-1} is related to Bi-O bending vibrations.[26] A less intense peak around 850 cm^{-1} is attributed to the bending vibration of Ba-O bond. [27] The calcined sample shows an absorption around 1446 cm^{-1}, which is due to the adsorption of atmospheric CO_2 during drying processes.

Adsorption studies
Since, the photo-assisted degradation of the dyes occurs predominantly on the photocatalystsurface,

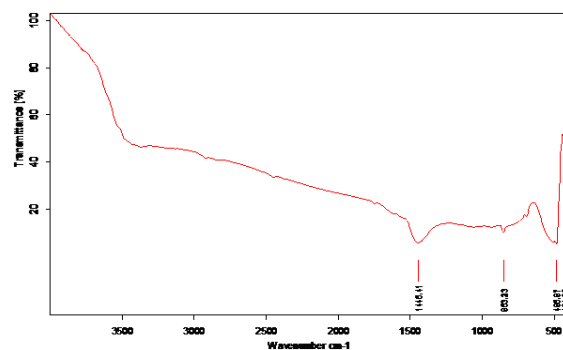studies on the adsorption of the dyes from aqueous solution onto

Figure 6. FTIR spectra of $BaBiO_3$perovskite

$BaBiO_3$ nanoparticles are relevant and important. Equilibrium adsorption data collected in the study are fitted on Langmuir adsorption isotherm[28]. Here in, we used the Langmuir model by assuming the monolayered adsorption phenomenon due to the presence of limited active adsorption sites. The linear form of Langmuir Isotherm is represented by the following equation:

$$\frac{Ce}{qe} = \frac{1}{Qob} + \frac{Ce}{Qo} \qquad (4)$$

where C_e is the concentration of the adsorbate (mgL^{-1}) at equilibrium.q_e is the amount of adsorbate per unit mass of adsorbent at equilibrium in mgg^{-1}. Q_o is the maximum adsorption at monolayer coverage in mgg^{-1}, b is the Langmuir adsorption constant in Lmg^{-1}. The plots of C_e/q_e versues C_e are linear and presented in Fig. 7. Langmuir adsorption constant (b) and the maximum adsorbable dye quantity (Q_o) are calculated from the intercept and slopes of this figure as 0.055 mgmL^{-1}0.334 mgg^{-1}, respectively. The correlation coefficient was found to be 0.917.
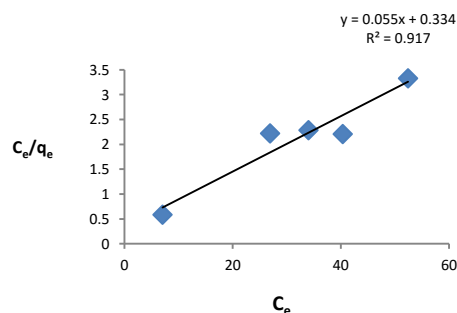

Figure 7. Linear transform of Langmuir isotherm [$BaBiO_3$=0.75gL^{-1}; pH=6.0]

Effect of catalyst loading
In order to avoid the use of excess catalyst, it is desirable to find out an optimum catalyst loading for efficient degradation. A series of experiments is carried out by

varying the amount of catalyst from 0.25 to 1.25 gL^{-1} at pH 6.0 and 50 mgL^{-1} MG concentration. It is observed that up to 0.75 gL^{-1} loading of photocatalyst degradation rate increases and then with further increase in loading, the rate decreases. The enhancement of removal rate may be due to the increase in the availability of active sites of the photocatalyst. When the concentration of $BaBiO_3$ catalyst increased above the limiting value the degradation rate decreased, due to the disruption of light by the suspension. Our results are in agreement with the earlier reports [8] Fig. 8 shows a plot of the degradation rate constant (K_{app}) as a function of the $BaBiO_3$ concentration at the fixed MG concentration (50 mgL^{-1}) and pH 6.0. Also, an empirical relationship between the initial dye concentration has been reported by Galindo et al ($r_o\alpha[catalyst]^n$ [dye]) , where n is a exponent less than 1 for all the dyes studied relative to low concentration of catalyst [29] As it can be seen in Fig. 9, the dependence of the $BaBiO_3$ concentration on the initial decolorization rate of MG follow a similar relationship

$$r_o\alpha[BaBiO_3]^{0.72} \text{ [MG]} \tag{5}$$

when the $BaBiO_3$ concentration is less than $1gL^{-1}$

Effect of pH
The effect of pH on the rate of degradation of dyes solution is investigated in the pH range 4.0-8.0 with
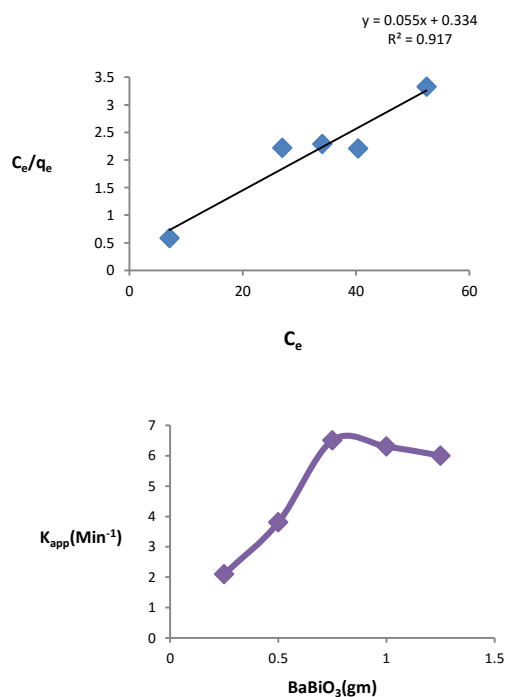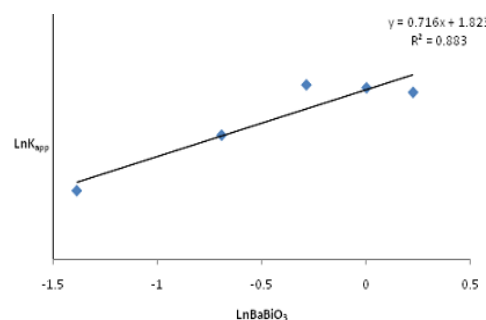
Figure 9. Relationship between LnK_{app} and the amount of $BaBiO_3$ [MG=50mgL^{-1}; pH=6.0]

constant catalyst loading of 0.75 gL^{-1} and 50 mgL^{-1} MG concentration. It is observed that the degradation efficiency increases with increase in pH upto 6.0 and with further increase in pH the degradation efficiency decreases. An increase in the rate of degradation with increase in the pH is due to the generation of more OH$^-$ ions. These ions loose an electron to the hole generated at the semiconductor surface and OH$^•$ free radicals are formed. These formed free radicals cause oxidation of the dye. On the further increase in pH above 6.0, a decrease is observed because at very high pH MG becomes negatively charged and so it repels negatively charged OH$^-$ions. This repulsive force does not allow the approach of OH$^-$ ions to the surface of catalyst and free radical generation is retarded. Fig. 10 shows a plot of the degradation rate constant (K_{app}) as a function of the pH .
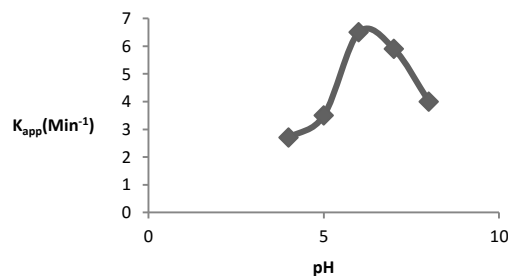
Figure 10. Effect of pH on the degradation rate [$BaBiO_3$=0.75gL^{-1}; MG=50mgL^{-1}]

Effect of initial dye concentration
The effect of the initial dye concentration of dye on the rate of degradation is studied by varying the initial dye concentration from 20to 80mgL^{-1} at pH 6.0, with a constant catalyst loading of 0.75gL^{-1}. It is observed that up to 50mgL^{-1} the degradation efficiency increases due to the greater availability of dye molecules for excitation and consecutive degradation, hence there is an increase in the rate. After this as the dye concentration is increased , the equilibrium adsorption of dye on catalyst surface increases; hence competitive adsorption of OH$^-$ on the same site decreases, which further decreases the rate of

Figure 8. Effect of $BaBiO_3$ loading on the degradation rate [MG=50mgL^{-1}; pH=6.0]

formation of OH⋅ radical, which is the principal oxidant necessary for a high degradation efficiency. On the other hand, considering Beer-Lambert law, as the initial dye concentration increases, the path length of photon entering the solution decreases, resulting in the lower photon adsorption on the catalyst particles and consequently a lower photodegradation rate [8].

In this work, we employed Langmuir-Hinshelwood model [21-22] to describe the total degradation of MG. L-H model covers both adsorption and photocatalytic phenomenon for explanation of dye degradation kinetics. The first order relationship for photocatalytic decomposition of dye can be represented as:

$$-\ln (C_0/C_t) = K_{app.}t \qquad (6)$$

where C_0, C_t and K_{app} are the initial dye concentration, concentration at time 't' and K_{app} is the apparent pseudo first order rate constant. The plots of $\ln(C_0/C_t)$ versus 't' with different initial concentration are shown in Fig. 11. The value of K_{app} is calculated by the slope of the above curves.

The value of initial degradation rate (r_o) is obtained by the multiplying the K_{app} values to the corresponding initial dye concentration, as follows;

$$r_o = K_{app.} C_o \qquad (7)$$

A linear expression can be conventionally obtained by plotting the reciprocal of initial rate ($1/r_o$) constant against reciprocal of initial concentration ($1/C_o$) (Fig. 12). The linear form of Langmuir–Hinshelwood kinetics can
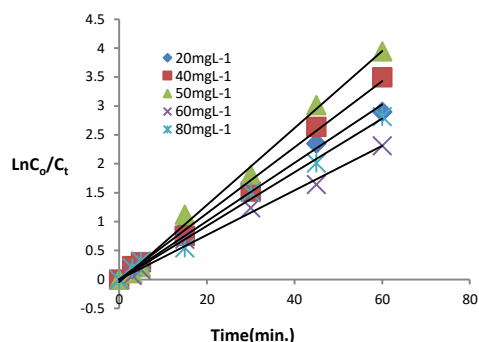

Figure 11. Effect of initial dye concentration on photodegradation of MG dye [BaBiO$_3$=0.75gL^{-1}; pH=6.0]

also be given by the following expression

$$1/r_o = 1/K_r + 1/K_r.K_{LH}.C_o \qquad (8)$$

here, K_r is the reaction rate constant and K_{LH} is the adsorption coefficient of the reactant also known as Langmuir-Hinshelwood constant. Table1 summarizes all the kinetic parameters calculated using the Langmuir–Hinshelwood model for dye degradation on using BaBiO$_3$ photocatalyst. K_r and K_{LH} values are 25.64 mgL^{-1}min.$^{-1}$, 1.42 Lmg^{-1} respectively. It is noteworthy that the Langmuir adsorption constant (b=0.055 Lmg^{-1}) obtained from the dark experiments are different from that determined by Langmuir-Hinshelwood equation (K_{LH} =1.42 Lmg^{-1}). This is due to the photoadsorption and very rapid photoreaction of the dyes on the catalyst surface [31].

Table 1. Influence of various parameters on visible light degradation of MG in BaBiO$_3$ suspension:

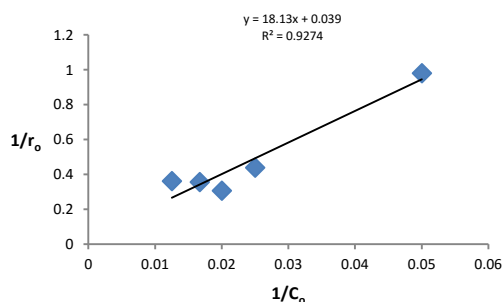| [MG]	BaBiO$_3$	pH	$K_{app}\times10^{-2}$	r_o	Kr	K_{LH}
mgL^{-1}	gL^{-1}		Min^{-1}	mgL^{-1}Min^{-1}	mgL^{-1}Min^{-1}	Lmg^{-1}
	0.25		2.1	1.05		
	0.5		3.8	1.9		
50	0.75	6.00	6.5	3.25		
	1		6.3	3.15		
	1.25		6	3		
20			5.1	1.02		
40			5.7	2.28		
50	0.75	6.00	6.5	3.25	25.64	1.42
60			4.6	2.76		
80			3.5	2.8		
		4.00	2.7	1.35		
		5.00	3.5	1.75		
50	0.75	6.00	6.5	3.25		
		7.00	5.9	2.95		
		8.00	4	2		

Figure 12. Langmuir-Hinshelwood plot of visible light degradation of MG in $BaBiO_3$ [$BaBiO_3$=0.75gL^{-1}; pH=6.0]

CONCLUSION

The synthesis of $BaBiO_3$ through Pechini method resulted in the formation of nanosized, mono phase crystalline material which has proved its potential as a photocatalyst in visible light owing to its low band gap of 2.07 eV. The photocatalytic activity and the corresponding degradation kinetics shows that it can efficiently degrade MG dye in the aqueous suspension under visible light irradiation. The dependence of the $BaBiO_3$ concentration on the initial degradation rate can be explained as ($r_o\alpha[BaBiO_3]^{0.72}$ [MG]), when the $BaBiO_3$ concentration is less than 1 gL^{-1} . The Langmuir adsorption constant (b) and the maximum adsorption at monolayer coverage Q_o are calculated as 0.055 Lmg^{-1} and 0.334 mgg^{-1} respectively .The photocatalytic degradation of MG by $BaBiO_3$is nicely fitted to the Langmuir-Hinshelwood kinetic model. The calculated values of the reaction rate constant (K_r) and Langmuir-Hinshelwood adsorption constant (K_{LH}) are 25.64 mgL^{-1}min^{-1}and 1.42 Lmg^{-1} respectively. Therefore, this simple technology of degradation of the colored effluents has the potential to improve the quality of the wastewater from textile and other industries.

Acknowledgements

REFERENCES

1. Galindo, C., P. Jacques and A. Kalt, 2001. Photochemical and Photocatalytic Degradation of an Indigoid Dye: A Case Study of Acid Blue 74 (AB74). Journal of Photochemistry and Photobiology. A: Chemistry. 141(1): 47-56.

2. Rao, K. V. K., 1995.Inhibition of DNA Synthesis in Primary Rat Hepatocyte Cultures by Malachite Green: a New Liver Tumor Promoter. Toxicology Letters, 81 (2-3), 107-113.

3. Alderman, D. J. and R. S. C. Hadley, 1993. Malachite Green: a Pharmacokinetic Study in Rainbow Trout, OncorhynchusMykiss (Walbaum). Journal of Fish Diseases. 16: 297-311.

4. Culp, S. J., F. A. Beland, R. H. Heflich, R. W. Benson, L. R. Blankenship, P. J. Webb, P. W. Mellick, R. W. Trotter, S. D. Shelton, K. J. Greenlees and M. G. Manjanatha, 2002. Mutagenicity and Carcinogenicity in Relation to DNA Adduct Formation in Rats Fed Leucomalachite Green, Mutation Research. 506/507: 55-63.

5. Schnick, R. A. 1988. The Impetus to Register New Therapeutants for Aquaculture. The Progressive Fish-Culturist, 50(4): 190-196.

6. Paninutti, L., N. Mouso and F. Forchiassin, 2006. Removal and Degradation of the Fungicide Dye Malachite Green from Aqueous Solution Using the System Wheat Bran-Fomes Sclerodermeus. Enzyme and Microbial Technology. 39: 848-853.

7. Mittal, A., D. Kaur and J. Mittal, 2009. Batch and Bulk Removal of a Triphenyl Methane Dye, Fast Green FCF, from Wastewater by Wastewater by Adsorption over Waste Materials, Journal Hazardous Materials, 163(2-3): 568-577.

8. Chen, C. C.; C. S. Lu, Y. C. Chung, J. L. Jan, 2007. UV Light Induced Photodegradation of Malachite Green on TiO_2 Nanoparticles. Journal of HazardousMaterial, 141: 520-528.

9. Suresh, T. and G. Annadurai, 2013. Synthesis, Characterization and Photocatalytic Degradation of Malachite Green Dye Using Titanium Dioxide Nanoparticles. International Journal of Research in Environmental Science and Technology, 3(3): 71-77.

10. Barakat, M. A., H. Schaeffer, G. Hayes and S. I. Shah, 2004. Photocatalytic Degradation of 2-Chlorophenol by Co-Doped TiO_2 Nanoparticles.Applied catalysis B: Environmental, 57: 23-30.

11. Sahoo, C., A.K. Gupta and A. Pal, 2005. Photocatalytic Degradation of Crystal Violet (C.I. Basic Violet 3) on Silver Ion Doped TiO_2 . Dyes and Pigments, 66(3): 189-196.

12. Mrowetz, M. W. Balcerski, A. J. Colussi and M. R. Hofmann, 2004. Oxidative Power of Nitrogen-Doped TiO_2PhotocatalystsUnder Visible Illumination. Journal of Physical Chemistry B, 108(45): 17269-17273.

13. Mrowetz, M., W. Balcerski, A. J. Colussi and M. R. Hafmann, 2004. Oxidative Power of Nitrogen Doped TiO_2Photocatalysts Under visible Light Illumination. Journal of Physical Chemistry B, 108(45): 17269-17273.

14. Kim, H. G., D. W. Hwang and J. S. Lee, 2004. An Undoped, Single-phase Oxide Photocatalyst Working under Visible Light. Journal of American Chemical Society, 126: 8912-8913.

15. Kudo, A., K. Omori and H. Kato, 1999. A Novel Aqueous Process for Preparation of Crystal from Controlled and Highly Crystalline $BiVO_4$ Powder. Journal of American Chemical Society, 121(49): 11459-11467.

16. Ramchandran, R., M. Sathiya, K. Ramesha, A. S. Prakash, G. Madras and A.K. Shukla, 2011. Photocatalytic Properties of $KBiO_3$ and $LiBiO_3$ with Tunnel Structures. Journal of Chemical Sciences, 123(4): 517-524.

17. Yu, K., S. Yang, C. Liu, H. Chen, H. Li, C. Sun and S. A. Boyd, 2012. Degradation of Organic Dyes via Bismuth Silver Oxide Initiated Direct Oxidation Coupled with Sodium Bismuthates Based Visible Light Photo Catalysis. Environmental Science and Technology, 46, 7318-7326.

18. Pechini, M. U. S. Patent No. 3.330.697 (11 July 1967).

19. Alemi, A., E. Karimpour, H.Shokri. 2008. Preparation, Characterization and Luminescent Properties of Europium Oxide Doped Nano LaMn$_{0.9}$Zn$_{0.1}$O$_{3+d}$ by Sol-gel Processing. Bulletin of Material Science, 31: 967-973.

20. Sverre M., G. Wang, M. A. Einarsrud and T. Grande, 2007. Decomposition and Crystallization of a Sol-gel-derived $PbTiO_3$ Precursor. Journal of American ceramic society, 90(8): 2649-2652.

21. Kumar, K. V., K. Porkodi, A. Selvaganapathi, 2007.Heterogeneous Photocatalytic Decomposition of Crystal Violet in UV Illuminated Sol-Gel Derived Nanocrystalline TiO₂ Suspension. Dyes and Pigment, 75: 246-249.

22. Senthilkumaar, S., and K. Porkodi, 2005. Heterogeneous Photocatalytic Decomposition of Crystal Violet UV-illuminated Sol-gel Derived Nanocrystalline TiO₂ Suspensions. Journal of Colloid and Interface Science. 288: 184-189.

23. Sunarso, J., S. Liu, Y. Lin and J.D. da Costa, 2009. Oxygen Permeation Performance of BaBiO₃₋δ Ceramic Membranes. Journal of Membrane Science, 344(1): 281-287.

24. Tang J, Zou Z, Jinhu Y, 2007. Efficient Photocatalysis on BaBiO₃ Driven by Visible Light. Journal of Physical ChemistryC, 111(34): 12779-12785.

25. Zhu, D. and Y. H. Zhang, 2002. Hydrothermal Synthesis of Single-Crystal La₀.₅Sr₀.₅MnO₃Nanowire UnderMild Conditions. Journal of Physics: Condensed Matter, 14(27): 519– 524.

26. Lee, C. Y., K. Y. Song and R. P. Sperline, 1996. Molecular Dynamics Simulation and Far Infrared Measurements of Ba₀.₆K₀.₄BiO₃. Korean Journal of Materials Research, 6(6): 555-560.

27. LAZAREVIĆ, Z. Ž, N. Ž. ROMČEVIĆ, J. D. BOBIĆ, 2009. Study of Ferroelectric BaBi₄Ti₄O₁₅ Obtained Via Mechanochemical Synthesis. Optoelectronics and Advanced Materials – Rapid Communications, 3(7): 700 -703

28. Mckay, G. 1982. Adsorption of Dye stuff from Aqueous Solution with Activated Carbon: Equilibrium and batch Contact Time Studies. Journal of Chemical Technology and Biotechnology, 32: 759-772.

29. Galindo, C., P. Jacques and A. Kalt, 2001. Photooxidation of the Phenylazonaphthol AO₂₀ on TIO₂: Kinetic and Mechanistic Investigations. Chemosphere, 45(6-7):997-1005.

Persian Abstract

چکیده

نانو ذره BaBiO₃ با روش Pechini آماده شده و خصوصیات آن با آنالیزهای SEM, XRD, FTIR, DT- TGA و UV DRS مشخص شد . مطالعات سنیتیکی جذب و پدیده تجزیه ، در تجزیه فوتو کاتالیستی رنگ سبز مالاکیت (Malachite) با استفاده از راکتور بسته تحت نور مریی، بررسی شد . آزمایش ها در یک سیستم فوتو کاتالیستی BaBiO3 معلق انجام شدند . اثر بارگذاری کاتالیست ، pH محلول و غلظت رنگ اولیه روی تجزیه رنگ بررسی شده اند. علاوه بر آن ، همچنین آزمایش جذب انجام شده است که نشان داده الگو جذب از مدل Langmuir پیروی می کند. تجزیه رنگ سبز مالاکیت (Malachite) از شبه سنیتیک درجه اول پیروی می کند و مکانیسم Langmuir-Hinshel Wood معتبر شناخته شد. پارامترهای سنیتیکی مختلف برای جذب و تجزیه فوتو کاتالیستی رنگ همچنین تعیین شد.